

Noise Emission From Various Shape Rods at Low-moderate Reynolds Number

Joanna Maria KOPANIA¹, Grzegorz BOGUSŁAWSKI

Corresponding author: Joanna Maria Kopania, email: joanna.kopania@p.lodz.pl

¹ Lodz University of Technology, 266 Piotrkowska Street, 90-924 Lodz, Poland

Abstract Aeroacoustic source localization is an important experimental tool and the first step to know the mechanism of noise generation. The flow around the various shape of rods is one of the major aeroacoustic noise source mechanism. Such rods represent simple models for technical applications like part of the landing gear of planes, train pantographs, antennas, vehicles part, ventilation system or bridge. The purpose of this paper is to clarify the influence of the rod shape in the noise generation mechanism in a low-moderate Reynolds number. In this work, the situation when various shape rods are in the area of laminar-turbulent flow was analyzed. The measurements were carried out for single circular, square, c-shape rods to study the noise effect depended on the Reynolds number. The measurements were performed on the specially constructed test stand with the outlet to the anechoic room. The 1/3 SPL differential spectrum as 2-D noise maps were obtained for studied rods. The acoustic differences between circular, square and U-beam rods were observed.

Keywords: noise, circular square rods, u-shape beam, sound pressure level

1. Introduction

Aeroacoustic sounds are the class of sounds that are generated by the movement of air passed objects or edges [1, 2]. A large number of studies are carried out for the flow around the various shape of objects because of the extensive variety of engineering and industrial applications, like bridges, buildings, antennas, vehicles and equipment [3-6]. These studies are important for understanding the underlying causes of the flow phenomena and also the strengths and weakness of available numerical models for finite geometries. The most studied flow configuration involves the circular or square cylinder inflow, where the flow is normal to the axis of the cylinder. In these cases, the vortices are in the process of the formation near the top of the cylinder surface, and the flow process in the wake of a cylinder involves the formation and shedding of vortices alternately from one side and then the other. The three-dimensional effects were identified, including the horseshoe vortex upstream of the cylinder, the base vortex, side-wall vertical vortices and tip vortices. This phenomenon is of major importance in engineering design because of the interchangeable formation and shedding of vortices, which create alternating forces, which occur more frequently as the velocity of the flow increases. In the case of the rectangular cylinder is also important to consider the effect of the L/D (length/width) ratio on the vortex shedding phenomena [7, 8]. The procedure of shape optimization for obstacles (4 Bezier curves) flow was also presented, as a cost function of acoustic power efficiency, which is derived directly from the fluctuations of the aerodynamic force [9].

The aeroacoustic sounds, in low flow speed, could be modelled by the summation of compact sources, which are known as monopoles, dipoles and quadrupoles. An acoustic monopole can be described as a pulsating sphere, much smaller than the acoustic wavelength. A dipole is equivalent to two monopoles separated by a small distance but of opposite phase. Quadrupoles are two dipoles separated by a small distance with opposite phases. Aeolian tones can be represented by dipole sources for the lift fundamental frequency. The Aeolian tone is virtually a single sine wave at low Reynolds numbers. When the Reynolds number increases, the vortices produce diffuses rapidly and the individual vortices merge into a turbulent wake. The wake produces wideband noise modelled by lateral quadrupole sources whose intensity varies with the eight power. The noise generated by a circular rod in a uniform or turbulent flow has been also studied [10-12]. The Aeolian tones from a single circular rod at high Reynolds (namely 2.5×10^5 to 2×10^6) were related

to the decrease and increase of the tone's amplitude in the super- and post-critical regimes to surface pressure fluctuation characteristics. The effect of free-stream turbulence on the vortex shedding noise from a single rod has also been studied but also more broadband nature of the vortex shedding noise in the presence of free-stream turbulence was identified.

Because there are use different member shapes in construction engineering, in this work, the various shape of rods (circular, square and u-beam rods) were studied at low- Reynolds number in wind tunnel by measurement of acoustics parameters. The circular and square rods were chosen as model ones. The noise emission of the studied model was determined. Obtained flow physics and acoustics properties have been analysed to understand the effects of aerodynamical noise of rods. The U-beam construction shape is widely used for example in urban rail transit vehicles due to its low structural height, lightweight properties, shape, and predicted lower noise generation. However, there is still insufficient research on the mechanism of noise radiation from this type of structure, also because of interactions between these objects and another in real conditions. It is difficult to analyze the noise field of such structures by analytical methods. These studies could be also referenced to the flow in the ventilation system - elements like grills, diffusers or slats have got also u-beam elements. In these systems, the low Reynolds numbers are often used, so it means that velocity does not exceed 5 m/s. This aspect was also taken into account in the present work.

2. Experimental method

The measurements were performed on the specially constructed test stand with the outlet to the anechoic room (Fig. 1). Airflow was induced by a fan mounted on the inlet of the stand and regulated by the power inverter. The anechoic test chamber is cubic, approximately 350 m³ in volume and has got walls that are acoustically treated with foam wedges reflecting a free environment.

The rods were supported by two vertical side plates that were mounted to the short sides of the nozzle. The shape and cross-area studied rods are presented in Fig. 2. Two circular rods were used - with diameters 10 mm and 16 mm. Also, the square rod was used, but with two configurations: when the shorter wall (10 mm) was opposite to the flow stream, and when the longer wall (15 mm) was opposite to the flow stream. The last rod used in this study was a u-beam, with two configurations: with the wall (25 mm) to the flow stream and with a u-shape/channel to the flow stream - description given in Fig. 3. The length of each bar was 350 mm.

The measurements of noise were made by using analyzer SVAN 958. The four microphones (M1, M2, M3, M4) were located at a distance of 500 – 600 mm above the rods, with the distance between microphones presented in Fig. 2. The microphones were calibrated before commencing the acoustic test. Microphones were used to measure noise in the flow field. When a microphone is located within an airflow field, it is recommended as best practice that a windscreen or nose-cone accessory should be used when taking acoustic measurements. In head-on laminar flow, the nose-cone accessory is the best choice. In all turbulent flow and parallel orientation laminar flow, the windscreen accessory is the best choice. In these studies, the microphones were located parallel orientation to flow streamline and were used in turbulent flow, so windscreens were placed on these microphones. The measurements were taken at a range of flow velocities between 3,0 m/s to 17 m/s (for studied rods range of Reynolds numbers was between $Re=3100 \div 18000$).

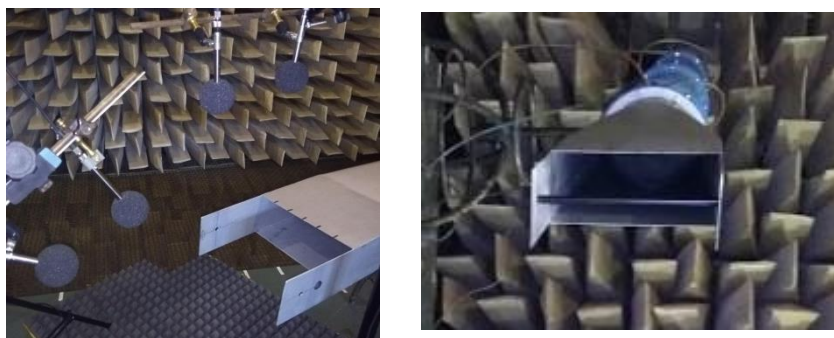


Fig. 1. The construction of the test stands with outflow to anechoic room and microphones.

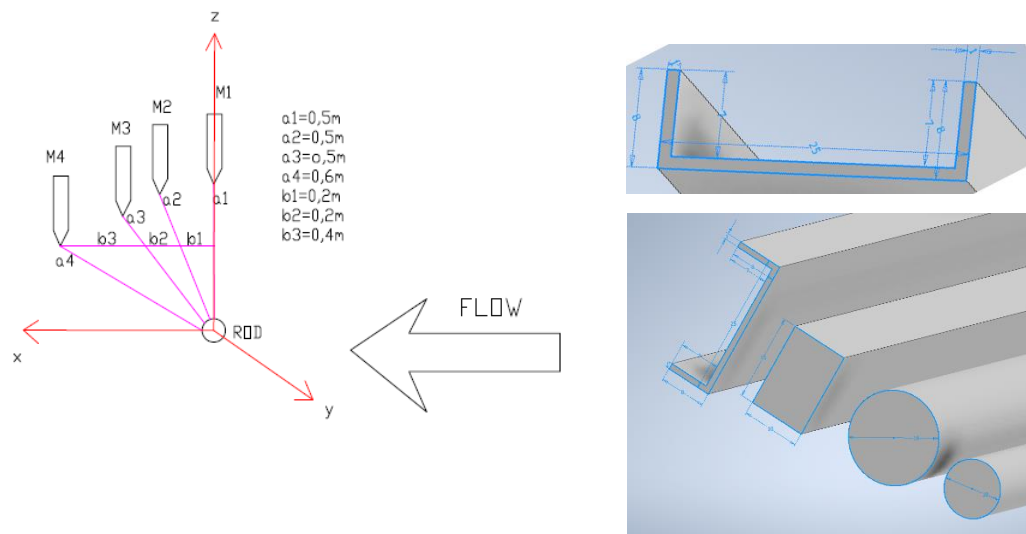


Fig. 2. Localization of microphones above the rods (on the left) and rods used in these studies (on the right) with zoom of U-beam. The length of each bar was 350 mm.

3. Discussion and results

Aeroacoustic parameters, like the sound pressure level of studied objects, are important for learning their physical nature. The attention of this work is focused on the flow-induced noise of studied rods. The vortex shedding generated by the cylinder is indeed responsible for a strong tonal noise at the frequency of the vortex shedding. The corresponding pressure field was studied in the anechoic room. The previous studies were provided for the circular rods [13]. Experiments have been performed to investigate the flow around circular rods with different diameter. The vortex shedding frequencies and flow velocity were measured for Reynolds numbers above 3000. The sound pressure level as a 1/3 octave spectrum and position of the dominant noise was highly dependent on the velocity. For studied circular rods, with diameters 10mm and 16mm, the maximum peaks at low frequencies were observed (from 100 Hz to 315 Hz) and move to higher frequencies along with the increase of the velocity of flow. In these studies, four microphones were used to measure the 1/3 octave sound pressure level (1/3 SPL). For circular and square rods a similar dependence was observed like in previous work [13] - for the M1 microphone (angle 0°). The colour-maps of 1/3-octave differential SPL spectrums were done to find the dependencies between velocities and observed peaks. In this work, the 1/3 differential SPL, determined as the difference between the 1/3 octave SPL spectrum of studied rods and background was examined, which eliminates other phenomena, which could influence on 1/3 octave SPL spectrum. The 2-D colour-maps were done by using bicubic interpolation depending on the obtained parameters for studied rods. The bicubic interpolation can achieve good performance because it assumes the smoothness of obtained data. Bicubic interpolation processes 4×4 (16 pixels) squares and is often chosen because of this, but it takes more time to process. For circular and square rods, the 1/3-octave differential SPL colour-maps were done for the range of frequency 40 – 500 Hz (Fig. 3), from the M1 microphone signals. As seen from these colour maps, the maximum peak (from microphone M1, red-pink colour area) is moving along the curve could be described by the linear-log model. Logarithmically transforming variables in a regression model is a very common way to handle situations where a non-linear relationship exists between the variables and such situation we often have got in acoustic measurements. For square rods, regardless of the length of the edge, the maximum peaks (at 160 Hz) are observed at the lower velocities. For square rod, the effect of an L/D (length/width) ratio on the vortex shedding phenomena is important [6]. For $L/D < 2 - 3$, such as for the studied square rod, in the one case the afterbody (length of geometry after separation point) is short and the upstream edge vortex shedding, dominates without impinging on the side-wall.

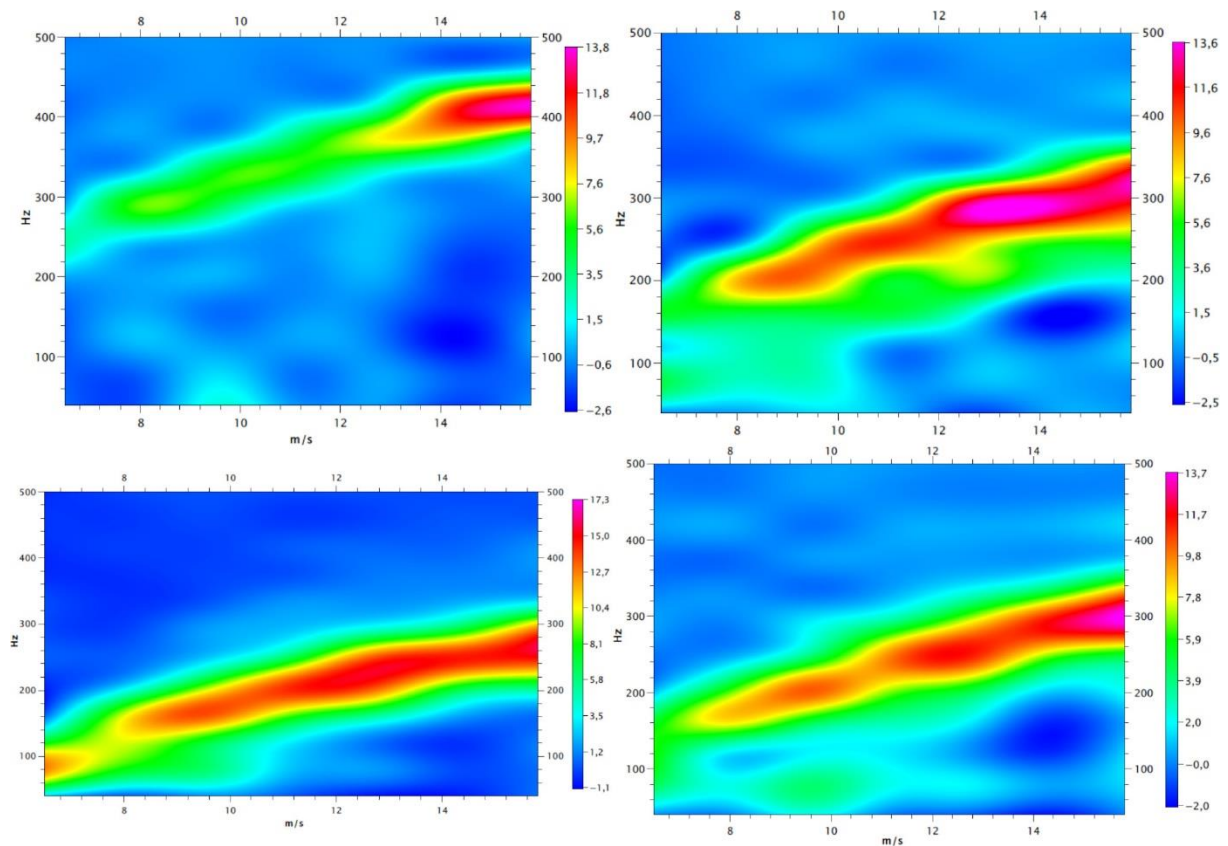


Fig. 3. The 1/3 differential SPL colour-map dependent on velocities measure by M1 microphone (on the graph: on the left-top for 10 mm rod; on the right-top for 16 mm rod; on the left-down for a square rod with 10 mm edge; on the right-down a square rod with 15 mm edge). The dB scale is shown by the bar on the right side of the graphs.

Instability waves and shear-layer vortices appear along with the separated boundary layers which have evolved from the front corners of the square rod. The shear layers present unsteady up/down “flapping” motions with the evolution of vortex shedding in the wake [14]. This effect probably gives a stronger acoustic signal at a lower velocity, than in the case of the circular rod. This correlation is not observed in the 1/3 SPL differential spectrum for the U-beam rod from the M1 microphone.

For the U-beam rod, the 1/3 SPL differential spectrum is observed from the M4 microphone (angle 48° to studied rods). The 2-D colour maps (Fig. 5) were done by using bicubic interpolation depending on the obtained parameters for square and U-beam rods. As seen from Fig. 4, the maximum peak for square rod (from microphone M4, red-pink colour area) is moving along the curve could be described by the linear-log model. But the maximum peak in the 1/3 SPL differential spectrum has got lower values than for the U-beam rod (around 2-4 dB). For U-beam rod the intensive maximum peak below 100 Hz is observed between 6 – 8 m/s. With increasing the velocity the maximum peak move to the higher frequencies. But it is not a gentle moving along the linear or logarithmic curve, but rather jumped movement to the next characteristic frequency region (around 200 Hz). If the U-beam rod was located u-shape to flow stream, the 1/3 SPL signal in whole frequencies region is taking higher values than for square rod. It is worth considering that the next peak appears around 300 Hz with the velocity increase. The flow around the stationary U-beam as the two periodic patterns are described thanks to the CFD simulations [15]. The fundamental difference between the two flow patterns lies in the behaviour of the free shear layer, separating from the U-beam at its top corner. This shear layer can either be curved weakly, giving rise to what will be called “R-flow” or it can roll up quickly, reaching into the cavity of the U-beam, giving rise to the so-called “U-flow”. The U-flow and R-flow pattern were be observed only in 2-D simulations (URANS).

However, the evolution of vortices can be highly three-dimensional, as is commonly known. To design experiments the flow pattern and employ flow visualization techniques is part of the ongoing research.

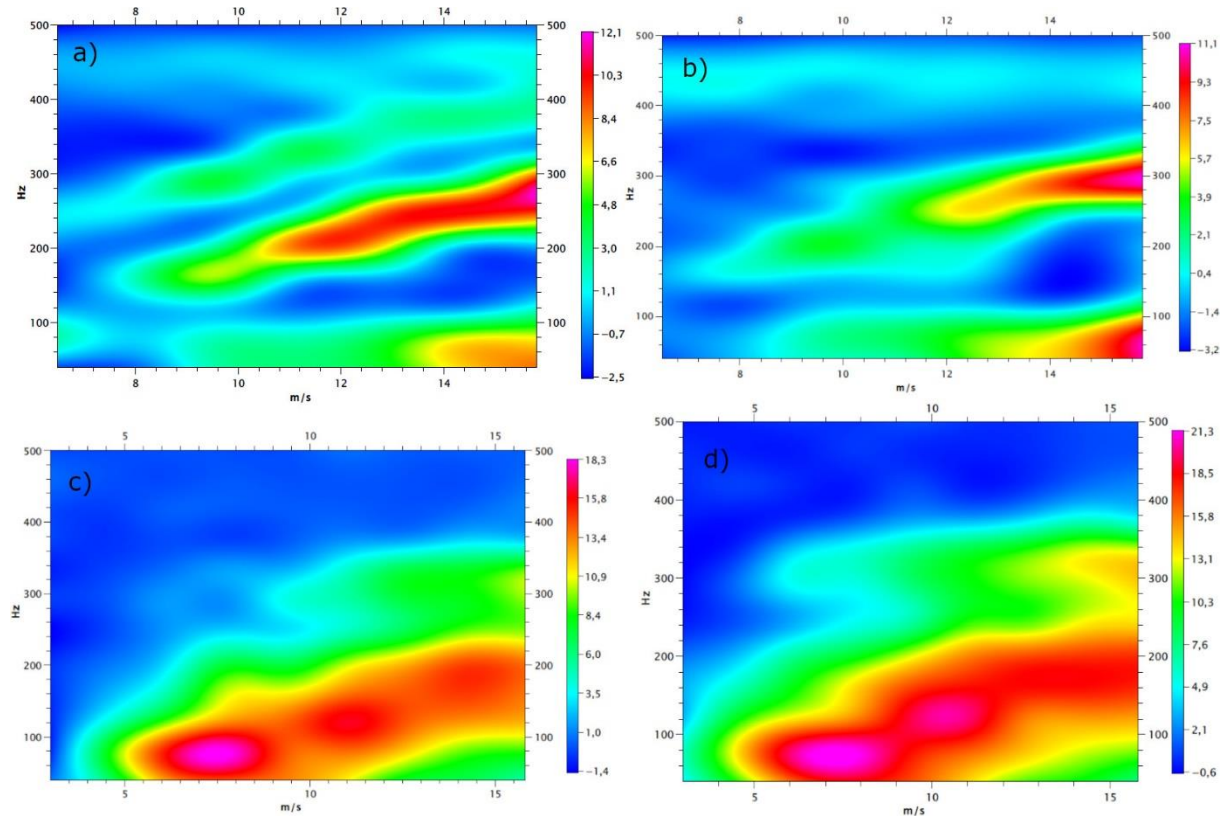


Fig. 4. The 1/3 SPL differential colour-map dependent on velocities measure by M4 microphone (on the graph: a) square rod with 10 mm edge; b) a square rod with 15 mm edge; c) U-beam rod with 25 mm edge; d) U-beam rod with the channel). The dB scale is shown by the bar on the right side of the graphs.

When the R-flow is realized, the free shear layer is curved weakly and extends into the wake behind the U-beam. Vortices form behind the U-beam is very similar to the flow around a full square rod. The stationary vortex in the cavity of the U-beam corresponds to the closed wall of the rectangular object. The aerodynamic forces acting on the U-beam vary sinusoidally with the vortex shedding. When the U-flow is realized the free shear layer is rolling up right behind the windward sidewall of the U-beam. This creates a large non-stationary vortex and a secondary vortex which separate from the sidewall and are advected through the cavity of the U-beam. This correlation probably was identified in Fig. 5, where 1/3 SPL colour-map dependent on velocities obtained from M3 microphone (angle 66°) is pictured.

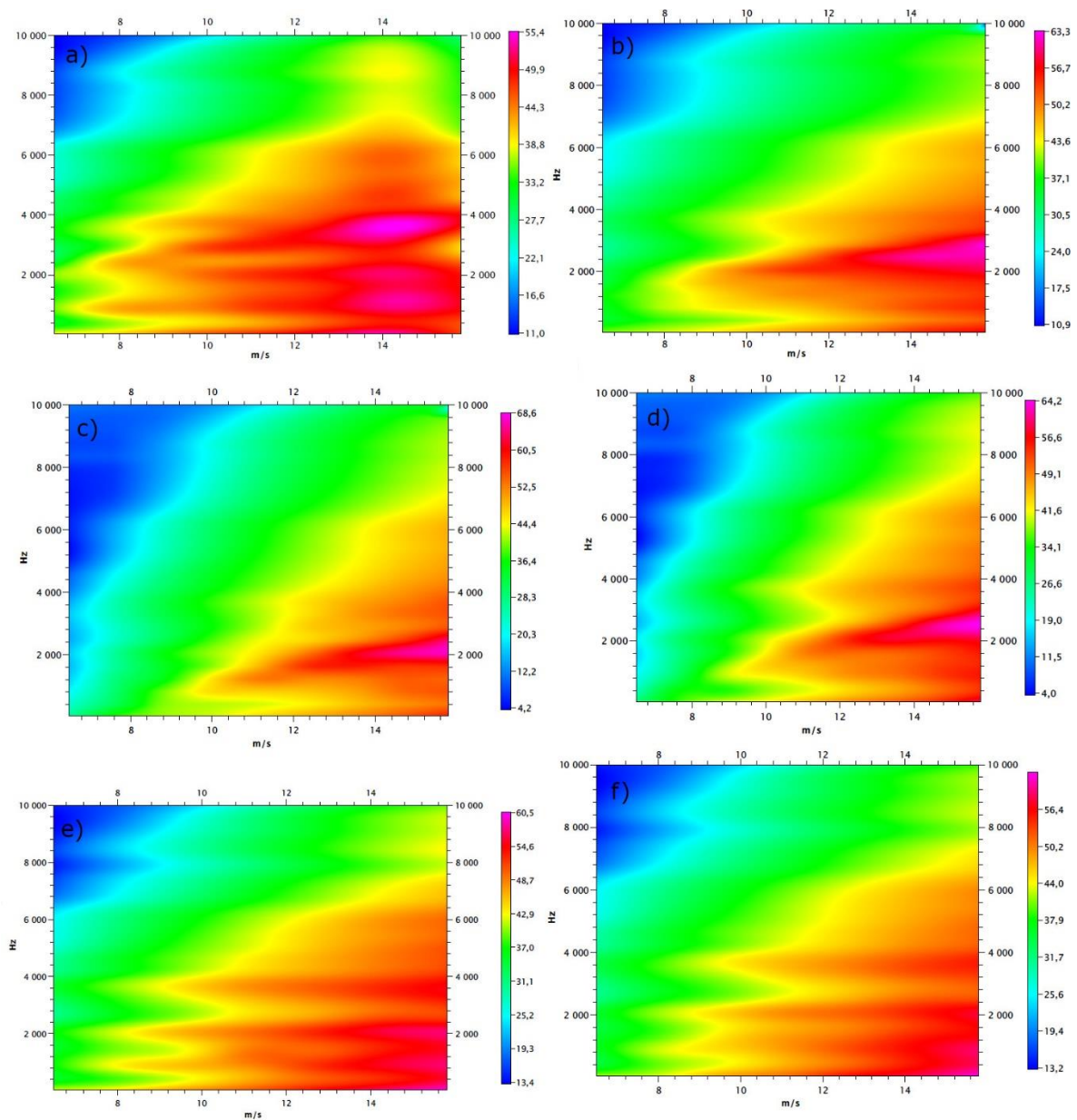


Fig. 5. The 1/3 SPL colour-map dependent on velocities measure by M3 microphone (on the graph: a) 10 mm diameter rod; b) 16 mm diameter rod; c) a square rod with 10mm edge; d) a square rod with 15 mm edge; e) U-beam rod with 25 mm edge; f) U-beam rod with the channel). The dB scale is shown by the bar on the right side of the graphs.

The 1/3 SPL spectrum shown that for square rods the acoustic signals have got the highest values (between 63-66 dB). For the circular and U-beam rods, the values of SPL are similar (around 55-63 dB). For the u-beam rod more peaks are observed (at 63 Hz, 125 Hz, 315 Hz, 1000 Hz, 2000 Hz, 4000 Hz - similar to the circular rod with a 10 mm diameter). These peaks merge when the flow velocity increase. However, to find out more information about the observed SPL signals and their correlation with flow pattern around the studied rods, aerodynamic measurements should be conducted (e.g. PIV).

4. Conclusions

This paper has reported the results of aeroacoustics measurements of the various shape of rods at $Re = 3100 - 18000$. The measurements provide some novel and important information regarding dependencies between the SPL signal and the velocity of the flow stream. For circular and square rods a similar dependence was observed. The 1/3 SPL differential colour maps show the maximum peak (from microphone M1, red-pink colour area) that could be described by the linear-log model. But for square rods, independent from the length of the edge, the maximum peaks are observed at the lower velocities. The maximum peak in the 1/3 SPL differential spectrum for the square rod has got lower values than for the U-beam rod. For U-beam rod the intensive maximum peak below 100 Hz is observed between 6 – 8 m/s. With increasing the velocity the maximum peak move to the higher frequencies, but the move is like a “jump” to the next characteristic frequency region. The acoustic signal U-beam could be connected with characteristic two patten flow around the stationary U-beam known as R-flow and U-flow. This research could give the inspiration for understanding the noise various shape of rods. To design new experiments that understand the flow around U-beam and linking it with the flow pattern the new flow visualization techniques should be used. However, the evolution of vortices can be highly three-dimensional, as is commonly known, so the simulation of CFD and acoustics could be preferred.

Additional information

The authors declare no competing financial interests.

References

1. R. Selfridge, J. D. Reiss, E. J. Avital. Physically derived synthesis model of an edge tone. 144th Audio Eng. Soc. Conv. 2018, 9956, 2018.
2. R. Selfridge, D. Moffat, E. J. Avital, J. D. Reiss. Creating real-time aeroacoustic sound effects using physically informed models. AES J. Audio Eng. Soc., 66(7-8):594-60, 2018. DOI:10.17743/jaes.2018.0033
3. C. H. K. Williamson. Vortex Dynamics in the Cylinder Wake. Annu. Rev. Fluid Mech., 28(1):477-539, 1996. doi:10.1146/annurev.fl.28.010196.002401
4. M. M. Zdravkovich, P. W. Bearman. Flow Around Circular Cylinders—Volume 1: Fundamentals. J. Fluids Eng., 120(1):216, 1998. DOI: 10.1115/1.2819655
5. M. Matsumoto. Vortex shedding of bluff bodies: a review. J. Fluids Struct., 13(7):791-811, 1999. DOI:10.1006/jfls.1999.0249.
6. T. M. Harms, G. Venter. Computational simulation of the turbulent flow around a surface mounted rectangular prism, 142:173-187, 2015. DOI: 10.1016/j.jweia.2015.03.019.
7. S. Deniz, T. Staubli. Oscillating rectangular and octagonal profiles: interaction of leading- and trailing-edge vortex formation. J. Fluids Struct., 11(1):3-31, 1997. DOI: 10.1006/jfls.1996.0065
8. G. Morgenthal. Fluid Structure Interaction Bluff-body Aerodynamics and Long-span Brige Design: Phenoma en Methods, tech. rep. University of Cambridge Department of Engineering, 2000.
9. W. Pinto, F. Margnat, W. José, S. Pinto, F. Margnat. A shape optimization procedure for cylinders aeolian tone, 2018. HAL Id : hal-01844771
10. H. Fujita, H. Suzuki, A. Sagawa, T. Takaishi. The aeolian tone characteristics of a circular cylinder in high Reynolds number flow. 5th AIAA/CEAS Aeroacoustics Conference and Exhibit, American Institute of Aeronautics and Astronautics, 1999.
11. M. R. Davis, N. H. Pan. Noise generated by the interaction of turbulent jets with circular cylinders. J. Sound Vib., 135(3):427-442, 1989. DOI: 10.1016/0022-460X(89)90697-4
12. W. Olsen. Noise generated by impingement of turbulent flow on airfoils of varied chord, cylinders, and other flow obstructions. 3rd Aeroacoustics Conference, American Institute of Aeronautics and Astronautics, 1976.
13. J. M. Kopania. Noise Radiation from Circular Rods at Low-Moderate Reynolds Number. Vibrations in Physical Systems, 30(1):2019116, 2019.
14. R. F. Huang, B. H. Lin, S. C. Yen. Time-averaged topological flow patterns and their influence on vortex shedding of a square cylinder in crossflow at incidence. J. Fluids Struct., 26(3):406-429, 2010. DOI: 10.1016/j.jfluidstructs.2010.01.003.

15. J. Strecha, H. Steinrück. Vortex Induced Vibrations of a U-beam under two different flow patterns. Proc. 8th Eur. Nonlinear Dyn. Conf., vol. C, 2014.

© **2021 by the Authors**. Licensee Poznan University of Technology (Poznan, Poland). This article is an open access article distributed under the terms and conditions of the Creative Commons Attribution (CC BY) license (<http://creativecommons.org/licenses/by/4.0/>).